Understanding the formation of supported lipid bilayers via vesicle fusion-A case that exemplifies the need for the complementary method approach (Review)

Lind, Tania Kjellerup; Cardenas Gomez, Marite

Published in:
Biointerphases

DOI:
10.1116/1.4944830

Publication date:
2016

Document version
Publisher's PDF, also known as Version of record

Biointerphases
A Journal of Biomaterials and Biological Interfaces

Understanding the formation of supported lipid bilayers via vesicle fusion—A case that exemplifies the need for the complementary method approach (Review)

Tania K. Lind and Marité Cárdenas

Citation: Biointerphases **11**, 020801 (2016); doi: 10.1116/1.4944830
View online: http://dx.doi.org/10.1116/1.4944830
View Table of Contents: http://scitation.aip.org/content/avs/journal/bip/11/2?ver=pdfcov
Published by the AVS: Science & Technology of Materials, Interfaces, and Processing

Understanding the formation of supported lipid bilayers via vesicle fusion—A case that exemplifies the need for the complementary method approach (Review)

Tania K. Lind
Nano-Science Center and Department of Chemistry, Copenhagen University, Copenhagen 2010, Malmö, 20506, Denmark

Marité Cárdenas[a)]
Nano-Science Center and Department of Chemistry, Copenhagen University, Copenhagen 2010, Malmö, 20506, Denmark and Department of Biomedical Sciences and Biofilm—the Research Center for Biointerfaces, Health & Society, Malmo University, 20500 Malmo, Sweden

(Received 19 January 2016; accepted 15 March 2016; published 31 March 2016)

In this review, the authors discuss the challenges of studying supported lipid bilayers (SLBs) deposited by vesicle fusion in terms of (1) evaluating SLB formation and quality using quartz crystal microbalance with dissipation and (2) analyzing the composition and asymmetry of SLBs composed by lipid mixtures using complementary surface sensitive techniques. An overview of the literature is presented and the inconsistencies on this topic are discussed with the objective to expand beyond simple lipid compositions and set the basis for forming and analyzing SLBs of complex natural lipid extracts formed via the vesicle fusion method. The authors conclude by providing some guidelines to successfully form SLBs of complex lipid mixtures including natural extracts.
[http://dx.doi.org/10.1116/1.4944830]

I. INTRODUCTION

Complex natural cell membranes are difficult to study in their native states. Simpler lipid model systems are therefore desirable for studying biomolecule interactions and/or the role of specific membrane components. Simple cell membrane models span from monolayers at the air–water interface to planar supported lipid bilayers (SLBs) and lipid vesicles of varying sizes, either tethered to a surface or in bulk solution. The appropriate choice of model system is dependent on the technique used for the study, and each of the model systems have advantages and disadvantages, which must be considered beforehand.[1–3] Lipid bilayers can be formed on solid supports using several techniques including Langmuir–Blodgett (LB) and Langmuir–Schaefer (LS) deposition,[4–6] lipid/detergent mixed micelles,[7,8] or vesicle fusion.[9–12] The latter two can be carried out *in situ*, while the LB/LS techniques require deposition of one monolayer at the time using a Langmuir film balance. This technique, however, is favorable for deposition of bilayers with a controlled and specific asymmetric leaflet composition,[6,13] something that is not otherwise possible using vesicle fusion or lipid/detergent micelles. An increasingly popular biophysical technique for preparing model cellular membranes is the Droplet Interface Bilayer method.[14,15] Here, the lipid bilayer is formed in between two water droplets that are submerged in oil and coated with a lipid monolayer. Since each droplet composition can be controlled, symmetric or asymmetric tailoring of the bilayer can be achieved.[16] Moreover, the aqueous solutions on either side of the membrane can also be controlled allowing for studies of the interactions between specific biomolecules and the membrane.[15,17] This method was recently used to reconstitute a lipid bilayer from the total extract of *Escherichia coli* as a model cell membrane.[15]

Compared to lipid vesicles, SLBs are more stable and their fixed and well-defined structures make them excellent model systems for a wide range of surface sensitive techniques. Under the right experimental conditions, high coverage SLBs are relatively easy to form via vesicle fusion. In this review, we focus on the vesicle fusion method to form SLBs and the challenges involved in producing and studying them as the lipid complexity increases. We present recommendations for protocols to form SLBs made of complex mixtures based on an overview of two often-used techniques to study the formation of SLBs: quartz crystal microbalance with dissipation (QCM-D) and atomic force microscopy (AFM). Moreover, an introduction to neutron reflection (NR) is included since this is an excellent complementary technique to probe the structure of buried interfaces in a nondestructive manner. Together, these three techniques can give a complete picture of vesicle fusion and the processes occurring at lipid membranes as discussed in Secs. III–VII.

II. SURFACE SENSITIVE METHODS TO STUDY SUPPORTED LIPID BILAYERS AND MOLECULAR INTERACTIONS WITH THEM

A. Quartz crystal microbalance with dissipation

The inherent piezoelectric properties of quartz are exploited in the QCM-D to induce oscillations in the sensor,

[a)]Electronic addresses: cardenas@nano.ku.dk; marite.cardenas@mah.se

which deforms when applied to an external voltage.[18] By alternating the voltage, a standing shear wave is generated between two gold electrodes. The crystal resonates when the quartz thickness is an odd integer of the wavelengths of the induced wave and the instrument therefore operates the crystal at odd numbered overtones. The quartz crystal is coated with a substrate of given properties, which is in direct contact with the solvent and thus constitutes the sensor surface.[19]

The shear wave decays evanescently into the liquid with a characteristic decay length, which is typically 250 nm for a crystal immersed in pure water and this is thus the effective detection range for the QCM-D.[20] A solvent is detected as a coupled mass with effective thickness corresponding to $\Delta\rho_L$, where ρ_L is the density of the liquid. The decay length varies with $\sqrt{\eta_L}$, where η_L is the absolute viscosity of the liquid. Therefore, if the solvent is exchanged with one of higher viscosity, it induces an increase in the effective thickness sensed by the crystal.[20] Shifts in frequency and dissipation can thus be observed upon (1) mass changes at the surface of the sensor and (2) changes of the solvent viscosity and density.

For thin, rigid, and homogeneous films, the principle behind the QCM-D is build on a simple relationship between change in mass and change in frequency of the sensor crystal. For such systems, the change in mass, Δm, is proportional to the frequency change, Δf, according to the simple Sauerbrey relation:[21] $\Delta m = -C \times \Delta f/n$, where n is the harmonic number and C is the material specific Sauerbrey constant given by: $C = t_q \times \rho_q/f_0$ with t_q being the thickness of the quartz, ρ_q the density of the quartz, and f_0 the main resonance frequency. For a common 5 MHz silicon crystal, the Sauerbrey constant equals -17.7 ng/cm^2. The dissipation of energy is measured as the dampening of the oscillations when the driving voltage to the crystal is shut off. The energy dissipation factor, D, is given by: $D = E_d/(2\pi E_s)$, where E_d is the energy dissipated during one period of oscillation and E_s is the energy stored in the oscillating system.[22]

For soft films, the Sauerbrey relation underestimates the mass change, and the film thickness must be deduced by fitting the simultaneously measured Δf and Δd data to a viscoelastic model by including a number of frequency and dissipation overtones.[22] Monitoring a number of overtones increases the sensitivity of the measurement and can give useful information on the deposited layers. The penetration depth of the overtones decreases with increasing overtone number. This implies that the high overtones are dissipated mostly within the adsorbed layer, while the low overtones mostly sense the bulk solution. The latter are thus often discarded in the analysis. Because of the varying detection range, simultaneous measurements of several overtones can give an estimate of the spatial distribution or homogeneity of the adsorbed layer as a function of distance from the surface.[23] The Maxwell model and the Voigt model are viscoelastic models implemented in QCM-D software (QTools by Q-Sense). These are simple mechanical models, which can be constructed by a (purely elastic) spring and a (purely viscous) dashpot in series or in parallel, respectively.[24,25] Moreover, there are model-free approaches to interpret QCM-D signals from soft and heterogeneous films based on the ratio of the Δf and Δd signals.[26]

Figure 1 exemplifies how the frequency (a) and dissipation (b) of a layer of adsorbed lipid vesicles compare to those of a continuous bilayer. The period of the oscillations [marked by two-headed arrows in Fig. 1(a)] is inversely proportional to the frequency, and the dissipation is a measure of how fast the oscillations decay upon stopping the electrical current to the sensor. When vesicles are residing on the sensor (red curves in Fig. 1), the frequency of the oscillations is low due to the added mass (this includes the water in the vesicle lumen) and the dampening of the oscillations is high due to the softness and compliance of the layer. When the vesicles fuse, they release a large amount of water and the resulting SLB is thin and well coupled to the surface. As a result, the frequency of the oscillations decreases while the decay time for the dampening of the oscillating signal increases (gray curves in Fig. 1). Each data point in the curves generated by the QCM-D during an experiment corresponds to the *change* of frequency or dissipation, Δf and Δd, respectively.

The QCM-D measures the *wet adsorbed mass* and not the *dry adsorbed mass* as other optical techniques such as ellipsometry, surface plasmon resonance, and reflectometry does.[28] This can be seen as an asset of the QCM-D technique, since it then constitutes a tool for acquiring complementary information on the adsorbed layer in different liquid environments and in combination with other surface sensitive techniques.[9,29]

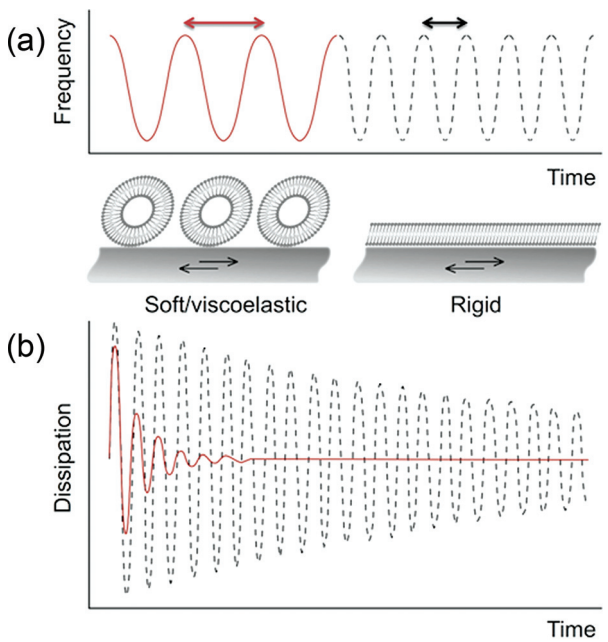

FIG. 1. Principle behind frequency and dissipation changes in the QCM-D. The graphs show examples of the frequency (a) and dissipation (b) signals generated from a soft vesicle layer (red curves) and a continuous lipid bilayer (gray curves). When the vesicles fuse, the frequency of the oscillations increases due to the formation of a well-defined bilayer and loss of coupled mass. In this context, a lipid bilayer is considered a rigid film because it is thin and fully coupled to the surface. The large dissipation of energy in the vesicle layer causes a significant dampening of the oscillations [red curve in (b)], so when the coupled water is released the dissipation decreases [gray curve in (b)]. The figure is redrawn based on inspiration from Ref. 27.

Indeed, this is the reason why QCM-D has become the method of choice to study SLB formation by vesicle fusion or molecular interactions at lipid bilayer interfaces.[23,30–34] However, the ability to sense the viscoelasticity of adsorbed layers can also in some cases severely complicate the interpretation of the data as for the vesicle fusion case, in particular.[12] In Secs. IV–VI, some examples will be discussed.

B. AFM and the setup for imaging under continuous flow conditions

In AFM, the surface topology is visualized via the interactions of a sharp tip and the resulting forces applied to the tip upon scanning the surface. The tip is integrated at the end of a flexible cantilever with an appropriate spring constant. A laser beam is focused at the apex of the cantilever and reflected onto a position sensitive detector [see Fig. 2(a)]. By scanning the surface in a raster pattern and detecting the laser beam position on the detector, an image of the structural features of the surface is generated in the computer. Depending on the type of material and the purpose of the study, the AFM can be operated in different modes, including contact, noncontact, or tapping (intermittent contact) mode.

In 1991, Zasadzinski and colleagues[35] were the first to employ liquid AFM imaging on a lipid bilayer (1,2-dimyristoyl-*sn*-glycero-3-phosphoethanolamine), and since then, a plethora of membrane studies have been conducted using the AFM. This technique provides knowledge on bilayer lateral organization, vertical distances, and various types of interactions with small molecules, etc. Since Zasadzinski and coworkers initiated this type of membrane studies, the AFM setup has been greatly improved and adjusted to the challenges of imaging soft biological samples. This includes the development of the TappingMode AFM imaging[36] and the PeakForce Quantitative Nanomechanical Property Mapping[37] technology. In particular, the latter method minimizes the forces applied to the sample, while enabling acquisition of mechanical properties of biological structures. In this way, images with information beyond topology (e.g., dissipation, adhesion, and modulus data) can be captured simultaneously.

In AFM experiments, solution exchange is complicated and can potentially alter the integrity of soft biological samples.[38] In the absence of a flow cell, the sample must be taken out and kept fully hydrated while exchanging the solution by adding and removing liquid several times (using a pipette, for example) followed by reinsertion of the sample in the AFM. When using a liquid cell, the solution exchange can be done using a syringe. Regardless of the approach, the tip must be disengaged during sample introduction. Standard protocols for imaging biomembranes and drug interactions involve a 10 min equilibration time in order to avoid thermal drift and to allow for refocusing of the laser, adjustment of the photodiode signal, and engaging the tip.[38] Furthermore, once a sample is reintroduced into the AFM, it is practically impossible to image the exact same spot that was imaged prior to disengagement. This may also be the case in a flow cell as small shifts, or drifts, can occur from the liquid exchange and from withdrawing and engaging the tip. This is a major challenge when studying complex processes taking place at biological interfaces, especially if the very initial steps of interaction happen within the equilibration time. These drawbacks obviously set limitations on the experimental outcome and make experiments hard to reproduce and interpret.

For these reasons, an AFM setup under continuous flow conditions (AFM-CFC) was developed. The major challenge of imaging under constant solvent flow is the extreme sensitivity of the cantilever and the tip to vibrations from the surroundings. Instead of using syringe injections, AFM-CFC utilizes a flow controlled by a slow gravity feed, which produces a continual flux and an environment stable enough for the cantilever to function and scan the surface without major drifts.[39] The optimized setup is sketched in Fig. 2(b). The slow feed is produced by careful control of the height difference between the sample and the outlets (1 and 5), allowing for a gentle flow through the cell. A very slow flux (a slightly nonlinear flow of 40–50 μl/min) can be obtained, in order to increase the spatial and time resolution. In this way, a sample solution can be pumped through the cell while the tip scans the surface allowing for high resolution imaging (for

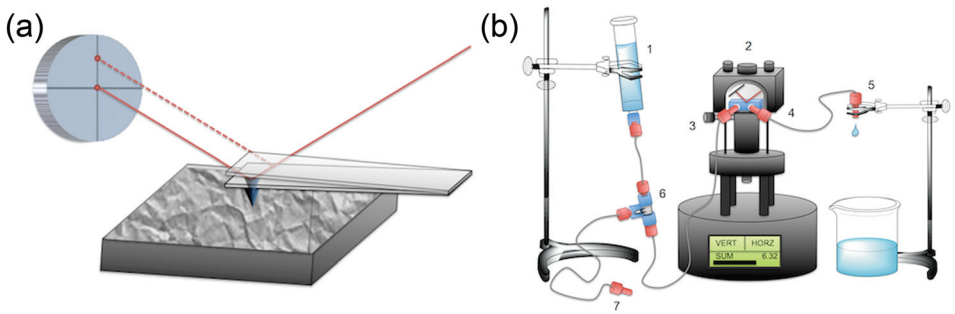

FIG. 2. (a) AFM utilizes the interatomic forces between a sharp tip and a surface in order to reveal topological features. The tip is integrated in a flexible cantilever that scans the surface in a raster pattern. A laser beam is aimed at the apex of the cantilever and reflected onto a position sensitive detector as illustrated. The changes in the position of the laser on the detector are converted into an image in the computer. (b) The optimized AFM-CFC setup is based on a gravity fed flow through the system. 1: the sample solution. 2: the scanning area where the flow cell is located. The cantilever is placed in the flow cell and a laser beam is focused on the apex and reflected onto a position sensitive detector via a mirror. 3 and 4: inlet and outlet of the flow cell. 5: the height of the outlet can be leveled to adjust the flow rate. 6: a three way valve that leads to a second outlet (7), which can be used either as a means for removing bubbles or to connect a second sample syringe.

example, using 512 × 512 pixel resolution and a scan rate of 1 Hz, ~8.6 min per image or 3–4 volumes exchanges of the flow cell per image) of, e.g., bilayer formation from vesicles adsorbing and fusing on the surface (see Sec. III) or biomolecule interactions with model membranes.[12,39] All the experimental steps including imaging of the clean surface, addition of sample, formation and rinsing of the membrane, and biomolecule interactions can then be performed *in situ* while maintaining a continuous flow of solvent over the surface. The advantages of imaging under flow conditions include that (1) no equilibration time is needed between injections (no thermal drift due to the continuous flow) allowing for imaging with no time delay, and (2) no shift in the imaged area is introduced by retracting and engaging the tip between injections. With this setup the very initial as well as the slower time-dependent surface interactions can be followed, as discussed in Secs. III and IV.

C. Neutron reflection

NR is a powerful technique for studying thin adsorbed layers, since it provides information on the structural features in the direction normal to the interface with a resolution down to a few Ångstrom. In this way, studies of buried interfaces that are otherwise difficult to probe can be carried out. For supported lipid bilayers, this means that the overall structure; layer thicknesses, lipid composition, and potential asymmetry between the leaflets can be characterized through a neutron scattering length density (SLD) profile, defined as

$$\mathrm{SLD} = \sum_i n_i(z) b_i,$$

where b_i is the neutron scattering length of nucleus i and $n_i(z)$ is the number density of nuclei i in the direction perpendicular to the interface.[7,40,41] The SLD profile is thus a continuous function of film depth, relating to the chemical composition of the adsorbed layer. The sensitivity of NR (change in reflectivity profile) depends on the difference in SLD of the molecules constituting the adsorbed layer and the solvent surrounding them. Besides their low irradiation damage and high penetration capabilities, one of the great advantages of neutron scattering is the large difference in neutron scattering length between hydrogen and deuterium that allows for noninvasively changing the SLD of the bulk solution or the sample. The latter can be achieved for instance by the use of specific deuteration of molecular entities. In this way, molecules can be tailor-made to have the same SLD as, for example, D_2O (D_2O matched), effectively making them invisible to neutrons in that specific solvent.[42] Moreover, labile hydrogen molecules in the sample will exchange spontaneously upon exchanging the bulk medium from H_2O to D_2O, thus slightly shifting the SLD of the sample. Finally, by tuning the H_2O to D_2O ratio and thereby the bulk SLD, any molecule can be made to disappear in solution. This phenomenon is called contrast variation, and it is one of the key advantages of neutron scattering in soft matter and biology. In order to obtain accurate fits of the NR data, it is crucial to get at least two different contrasts, but more may be needed depending on the complexity of the system. Potential compositional differences within the SLB can be revealed by NR using the contrast variation method as discussed in Sec. V.

In specular NR (with reference to an everyday mirror), the angle θ_i, of the incident wave vector $\mathbf{k}_i$ with the surface equals the angle, θ_r, of the reflected wave vector $\mathbf{k}_r$, as depicted in Fig. 3(a). The lengths of the incident and the reflected wave vectors are equal and given by

$$|\mathbf{k}_i| = |\mathbf{k}_r| = \frac{2\pi}{\lambda},$$

where λ is the wavelength of the neutron beam. The change in $\mathbf{k}$ on reflection of the surface is thus given by

$$|\mathbf{k}_r - \mathbf{k}_i| = 2|\mathbf{k}_{i\perp}| = \frac{4\pi}{\lambda}\sin\theta = Q_z = Q,$$

where

$$|\mathbf{k}_{i\perp}| = \frac{2\pi}{\lambda}\sin\theta$$

is the length of the component of $\boldsymbol{k_i}$ normal to the interface as defined in Fig. 3(a). This quantity is the length of the component of the momentum transfer normal to the interface. It is

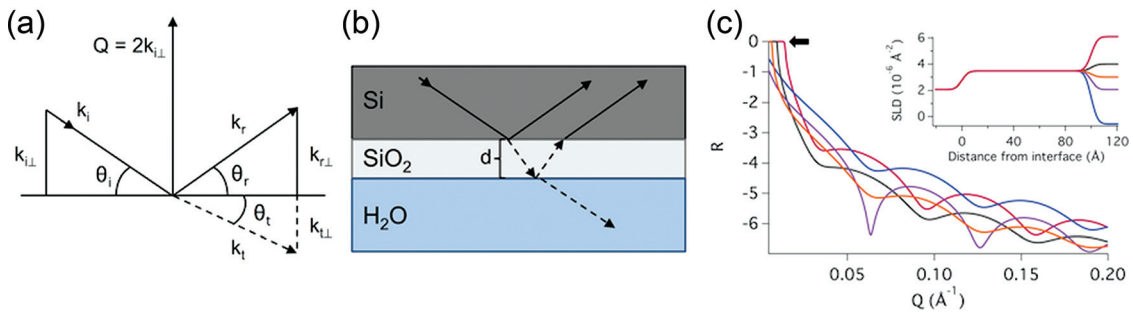

FIG. 3. (a) Sketch of a neutron beam impinging on a surface with definitions of the incoming, reflected, and transmitted wave vectors ($\mathbf{k}_i$, $\mathbf{k}_r$, and $\mathbf{k}_t$, respectively) their angles with the surface ($\theta_i = \theta_r$ and θ_t) and the scattering vector Q. (b) Illustration of neutron scattering from a silicon block with a thin layer of native silicon oxide of thickness d facing bulk H_2O. (c) Simulated reflectivity curves of a layer of silicon oxide on silicon in five different bulk contrasts—blue: H_2O, purple: 40 v/v% D_2O, orange: 50 v/v% D_2O, gray: 60 v/v% D_2O red: pure D_2O. The black arrow marks the critical edge of the D_2O contrast. A natural silicon oxide layer on silicon ⟨111⟩ is usually 5–30 Å thick, but in this graph, it is modeled as being 100 Å thick to exaggerate the Kiessig fringes. The inset in (c) gives the SLD profile in the direction perpendicular to the interface. The SLD profiles are not sharply defined due to interfacial roughness.

denoted Q_z and called the scattering vector. The data acquired in a neutron reflection experiment are normally displayed as the reflectivity as a function of Q_z as shown in Fig. 3(c) for a 100 Å thick SiO_2 layer on Si in different isotopic solvent contrasts [Fig. 3(b)]. The reflectivity is given by the relative intensity I/I_0 of the reflected beam, where I is the number of neutrons reflected at Q_z and I_0 is the number of incident neutrons. Specular x-ray reflection is an alternative technique that can give very useful and complementary information to neutron reflection, since x-rays present a linear dependency with electron density. Besides specular neutron/x-ray reflection, there are other techniques that focus on the off-specular scattering and grazing incidence small angle scattering (GISANS/GISAXS referring to neutrons and x-rays, respectively). These techniques give valuable structural information on lateral structures from nanometer to micrometer scale (for relevant reviews see, for example, Refs. 40 and 43). With regards to x-rays, the main limitation is that a biological sample has poor scattering contrast on a solid substrate, and therefore, it is often not possible to detect SLBs on solid substrates.[44]

III. FORMATION OF SUPPORTED LIPID BILAYERS BY VESICLE FUSION, THE CASE FOR SINGLE COMPONENT AND FLUID LIPID SYSTEMS

As discussed previously, QCM-D is an extremely sensitive technique especially for viscous layers that contain large amounts of water as vesicles do. This is why QCM-D has become a stronghold for studying SLB formation via vesicle fusion.[30] AFM, on the other hand, excels for in-plane imaging of the morphology of an adsorbed layer with lateral resolution down to a few nanometer and Ångstrom resolution in the vertical direction. The use of the AFM-CFC setup enables *in situ* imaging of layers during deposition. Finally, NR is very sensitive to buried interfaces but less sensitive to diffuse water-rich structures such as vesicles. Together these techniques are valuable for understanding the process of vesicle fusion and the structure of supported lipid bilayers as discussed in Secs. V–VI.

The adsorption and spreading of phosphatidylcholine (PC) vesicles have been extensively studied by QCM-D (Refs. 9, 10, 30, and 45) and the expected Δf and Δd values are well characterized for simple PC bilayers above the lipid melting temperature. Briefly, due to the added mass the frequency of the sensor decreases once the vesicles adsorb to the surface. Simultaneously, the energy dissipation increases because of the softness and viscoelasticity of the vesicles. It has been proposed that once a critical density of vesicles have attached to the surface, they become unstable and eventually break to form a continuous bilayer.[46] As this happens, Δf increases consistent with a loss of mass due to the release of water from the vesicle lumina while Δd decreases due to the formation of a thin, homogeneous membrane, which is more rigid and well-coupled to the surface as compared to a vesicle layer. The characteristic QCM-D traces of the formation of a dipalmitoylphosphatidylcholine (DPPC) bilayer in the fluid phase (50 °C) are shown in Fig. 4(a) (dashed lines).[12] These responses are similar to 1-palmitoyl-2-oleoyl-phosphatidylcholine (POPC) bilayer formation at room temperature.[30] However, in general, the processes of vesicle fusion and bilayer formation are highly dependent on the solution conditions used for dispersing the lipids, even for simple PC vesicles in the fluid phase.[47] As an example, the dashed curves in Fig. 4(a) show deposition in phosphate buffered saline (PBS) solution with an ionic strength of 100 mM NaCl, whereas the full lines show vesicle fusion in ultrapure water.[48] In the latter case, no distinct frequency minimum is observed, suggesting that the vesicles spread on contact with the surface, without the buildup of a critical surface coverage of vesicles before rupture and fusion. Interestingly, using the AFM-CFC technique the formation of an SLB containing 80 mol. % DPPC and 20 mol. % POPC could be imaged *in situ* in pure water. The images showed how the vesicles fused upon reaching the mica surface until a complete, phase-separated SLB of high quality was formed [Fig. 4(b)].[48]

The overall appearance of the QCM-D responses and whether or not a critical surface coverage is reached before vesicle rupture can be influenced, e.g., by the ionic strength,

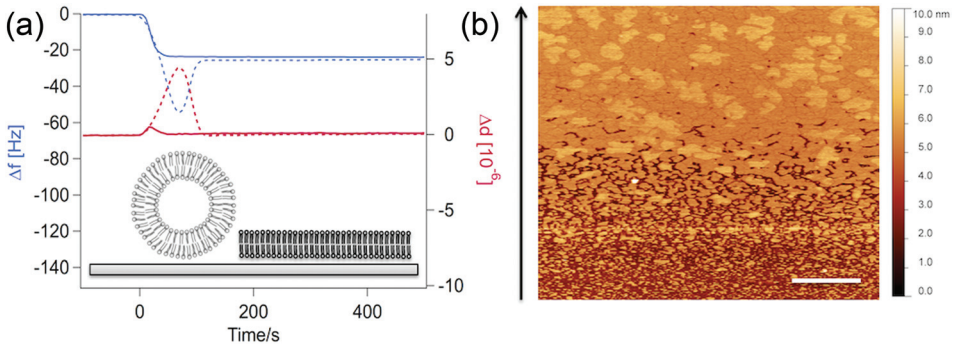

FIG. 4. (a) Graph shows Δf (blue) and Δd (pink) upon adsorption, fusion and spreading of vesicles composed of pure DPPC in the fluid phase (50 °C, flow rate of 100 μl/min). The vesicles were prepared in either PBS (dashed lines) or in ultrapure water (full lines). Depictions in the lower part of the graph show how the lipids are distributed during the process of membrane formation in PBS. (b) Image of an 80 mol. % DPPC 20 mol. % POPC membrane during bilayer formation in ultrapure water using the AFM-CFC technique (25 °C, 50 μl/min, 512 × 512 pixel resolution, and scan rate of 1 Hz). The image was scanned along the direction of the arrow under continuous flow of lipid vesicles. Initially, small bilayer patches appear. With time, they grow in size and eventually fuse to form a complete, defect-free membrane, which exhibits both a fluid and a gel phase (taller, brighter domains). The white scale bar is 1 μm.

presence of divalent cations, *p*H, temperature, and lipid concentration.[46] However, as long as the vesicles do rupture, the kinetics of the process does not seem to be crucial for the quality of the resulting membrane in terms of coverage and structure. Full SLB coverage corresponds to Δf and Δd values of -25 Hz and 0 for POPC and/or DPPC bilayers, respectively.[12,34] More negative values of Δf and more positive values of Δd are indicative of coadsorbed vesicles, while less negative values of Δf suggest reduced bilayer coverage. It should be noted that there is no universal recipe for bilayer formation using vesicle fusion. In general, the nature of the lipids, the surface properties and the solution conditions determine the outcome of vesicle fusion and bilayer formation. Recently, a careful study on the effect of vesicle size on the QCM-D signal was published in which a critical vesicle size was found to give optimal signals for vesicle fusion.[47] The authors used extrusion to produce vesicles of different sizes ranging from 90 to 160 nm in average hydrodynamic diameter in a phosphate buffered saline solution. They concluded that under these conditions even in the case of simple systems containing one lipid in the fluid phase, SLBs with the expected QCM-D traces for vesicle-free bilayers could only be formed below a certain vesicle size threshold ($\leq$90 nm in average hydrodynamic diameter). Different vesicle size populations can be produced when using tip sonication. The size distribution depends on the sonication time, the lipid composition (presence of charges, etc.) the ionic strength and screening capability of the buffer. When lipids are dissolved in buffer longer sonication times are expected in order to produce clear vesicle solutions as compared to samples prepared in pure water. For prolonged sonication times, it is important to use a water bath in order to reduce the heat produced and to keep the lipids at a constant and controlled temperature.

Fluid phospholipids and mixtures of fluid phospholipids containing cholesterol are typically considered nonvesicle fusing systems on gold substrates as evaluated by QCM-D.[30,49] However, a neutron reflection study clearly showed that dimyristoylphosphatidylcholine (DMPC)/cholesterol vesicles fused to form SLBs of high quality on gold.[44]

These cases highlight the need for complementary techniques in order to conclude with certainty whether or not a bilayer is formed or if vesicles are coadsorbed with a bilayer structure or form a complete supported lipid bilayer, see Sec. IV for a discussion on these issues.

IV. SUPPORTED LIPID BILAYERS CAN BE FORMED BELOW THE MELTING TEMPERATURE USING THE VESICLE FUSION METHOD

It is a general conception within the lipid membrane scientific community that lipid bilayers have to be formed above the main transition temperature.[30,38,47,50] Some publications include structural studies of membranes in the gel phase (formed above T_m followed by cooling),[51] but information on lipid bilayer formation via vesicle fusion below the main lipid transition is extremely scarce.[46,47,50] Several studies on vesicle adsorption and bilayer formation investigated the effect of surface chemistry (SiO_2 vs TiO_2),[34,52] vesicle size,[34,47,52] lipid concentration,[46,53] deposition temperature,[34,47,50] or osmotic pressure.[34,47] As an example, Seantier *et al*. studied vesicle fusion of lipid mixtures at temperatures close to the phase transition.[46,50] The authors observed SLB formation in the AFM at 9° below the T_m of an equimolar mixture of DMPC and DPPC showing that these lipid mixtures could form SLBs of high quality in the gel phase. However, the authors concluded that SLB formation was incomplete due to the large signals observed for Δf and Δd in the QCM-D and that complete bilayer formation on silica occurs only for temperatures above the T_m of the mixture.[46] We studied the effect of temperature on the formation of SLB by vesicle fusion of DPPC vesicles below and above the lipid T_m.[12] When lipid vesicles composed of pure DPPC were adsorbed on a silica surface well above the lipid T_m, the QCM-D responses for Δf and ΔD appeared as expected for successful bilayer formation, i.e., similar to fluid POPC bilayers formed at room temperature [Fig. 5(a), full lines]. Although, large signals were observed for Δf and Δd if the temperature was decreased below the T_m indicating a massive increase in adsorbed mass and the formation of a very soft and viscous film, dissipating a large amount of energy [Fig. 5(a), broken lines]. These findings were in accordance with previous reports,[47] and the signals are usually related to adsorption of intact vesicles,[52] which do not fuse to form an SLB.

Using the optimized AFM-CFC setup, it was possible to directly visualize the process of bilayer formation below T_m [Fig. 5(b)]. The gel phase vesicles fused and spread immediately on contact with the solid support followed by further vesicle adsorption on top of the SLB. Some of these vesicles could be removed by slowly rinsing with PBS under continuous flow during imaging whereas hot PBS, injected manually by syringe at an increased flow rate, successfully removed the remaining vesicles. Seantier *et al*. discovered that close to the T_m the kinetics of bilayer formation were significantly impeded.[50] The authors used a traditional liquid AFM imaging setup with a fixed volume injection and in order to obtain complete bilayer formation they had to apply a second injection of lipid solution. Due to these findings, the authors considered bilayer formation using mixtures of higher DPPC content unfeasible. With the AFM-CFC method sufficient mass transfer from the solution to the surface can be ensured, and this approach therefore closer resembles the conditions used for QCM-D and other *in situ* techniques such as NR. Indeed, NR confirmed the presence of a bilayer for depositions both above and below the lipid T_m and, interestingly, the coverage was higher for the membrane deposited in the gel phase [87 vs 68 ± 3 v/v% (Ref. 12)]. This can be explained simply by taking into account the increased area per molecule for fluid lipids; when the membrane is deposited in the fluid phase and then subsequently cooled down to below the T_m, the bilayer shrinks, effectively inducing defects in the membrane.[51]

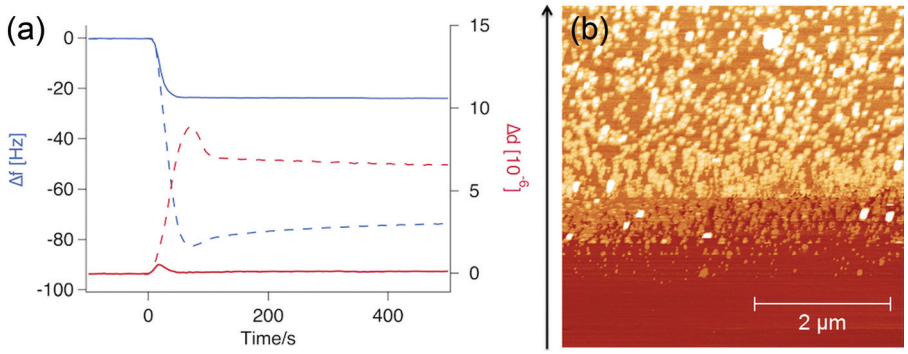

FIG. 5. Formation of supported bilayers by vesicle fusion of gel phase DPPC lipids—(a) Δf (blue) and Δd (pink) changes for bilayer formation of DPPC at 50 °C (full lines) and at 25 °C (broken lines) in ultrapure water. (b) AFM image of the formation of a gel phase DPPC membrane. The image was obtained using the AFM-CFC technique and was captured in ultrapure water in the direction along the arrow. Adapted with permission from T. K. Lind, M. Cardenas, and H. P. Wacklin, H. P., "Formation of supported lipid bilayers by vesicle fusion: effect of deposition temperature," Langmuir **30**(25), 7259–7263 (2014).

From these studies, it is clear that SLBs can be prepared from fusion of lipid vesicles below the main transition temperature. However, the issue of SLB formation via vesicle fusion is much more complex. For instance, heterogeneous mixtures that sometimes have multiple phase transitions, the presence of charged lipids and thus the need for fusion promoters, the preparation of the vesicles in terms of size distribution, buffer type, and ionic strength are all parameters that govern how the sensitive responses of the QCM-D will appear. Indeed, the presence of a small amount of vesicles coadsorbed at the interface will lead to high frequency and dissipation values whether they are adsorbed on the surface as a vesicle layer, in bilayer defects or on top of an intact SLB. This was confirmed by NR, where 14 ± 2 v/v% vesicles were detected on top of the SLB formed below T_m.[12] Hence, it is apparent that QCM-D data may be unclear with regards to whether an SLB is formed or not. If the quality of lipid bilayers is assessed using QCM-D, the data must therefore be carefully interpreted and preferably combined with complementary techniques to avoid misleading conclusions since the presence of coadsorbed vesicles does not in any way affect the structure of the underlying SLB.[51] For biomolecule interaction studies, any excess or coadsorbed vesicles should be minimized by careful rinsing of the membrane and in some cases by applying osmotic pressure shock or hot water rinses.[54] Indeed, the apparent lack of successful bilayer formation on substrates such as gold or titanium reported in the literature might also be a consequence of the methods used to probe the fusion process.[30,44]

V. SUPPORTED LIPID BILAYERS DO NOT NECESSARILY HAVE THE SAME COMPOSITION AS THE VESICLES THEY ARE MADE FROM

In the case of binary lipid mixtures, favorable interactions between a given lipid type and the surface might lead to bilayer asymmetry and/or SLBs with compositions that differ from the bulk vesicle composition. The issue of composition and asymmetry resulting from vesicle fusion of binary phospholipid mixtures has been discussed in the past.[11,55–59] These publications raised an important question on whether or not the solid support itself could significantly alter the composition and structure of a membrane upon fusion of mixed vesicles.[55,56] In general, specific interactions between the support and the proximal leaflet, surface-induced impeded lipid mobility or an inherent heterogeneous distribution of lipids in the mixed vesicles at the single vesicle level are all factors that could contribute to such effects.[11] When lipid membranes are composed of more than one lipid species, the overall structure of the membrane will depend on the properties of the lipids involved and the ratio between them. Here, the POPC and DPPC mixture is presented as an example since these lipids present similar molecular volumes but significantly different main transition temperatures (−2 and 42 °C, respectively). They are thus in different physical phase states at room temperature; POPC is fluid while DPPC is gel-like. For POPC and DPPC mixtures, the formation of a single lipid phase is only obtained at certain molar ratios and in specific temperature intervals. The mixtures that were included in the study covered four molar ratios that, according to the bulk phase diagram,[60,61] will produce membranes ranging from fluid (0 and 20 mol. % DPPC) to gel phase (100% DPPC), while crossing the two-phase coexistence regime (50 and 80 mol. % DPPC) at room temperature [see Fig. 6(a)]. In the coexistence regime, the lamellar structure presents phase separation, where gel-like domains enriched in DPPC are surrounded by a fluid phase enriched in POPC. The fluidity and lateral organization of the membranes were probed by fluorescence recovery after photo bleaching and AFM imaging and reflected the bulk phase diagram.[11] Clear phase separation occurred for 80 mol. % DPPC with a 10 Å thickness difference between the fluid and gel phases in accordance with previous results.[11,62]

The transbilayer distribution of lipids was studied by NR utilizing mixtures of hydrogenated and tail-deuterated lipids and by taking advantage of the concept of bulk contrast variation for improved resolution. Interestingly, in all cases, the bilayers were overall enriched in POPC as compared to the nominal composition of the vesicles [Fig. 6(b)]. The maximum deviation was found for the fluid, single-phased

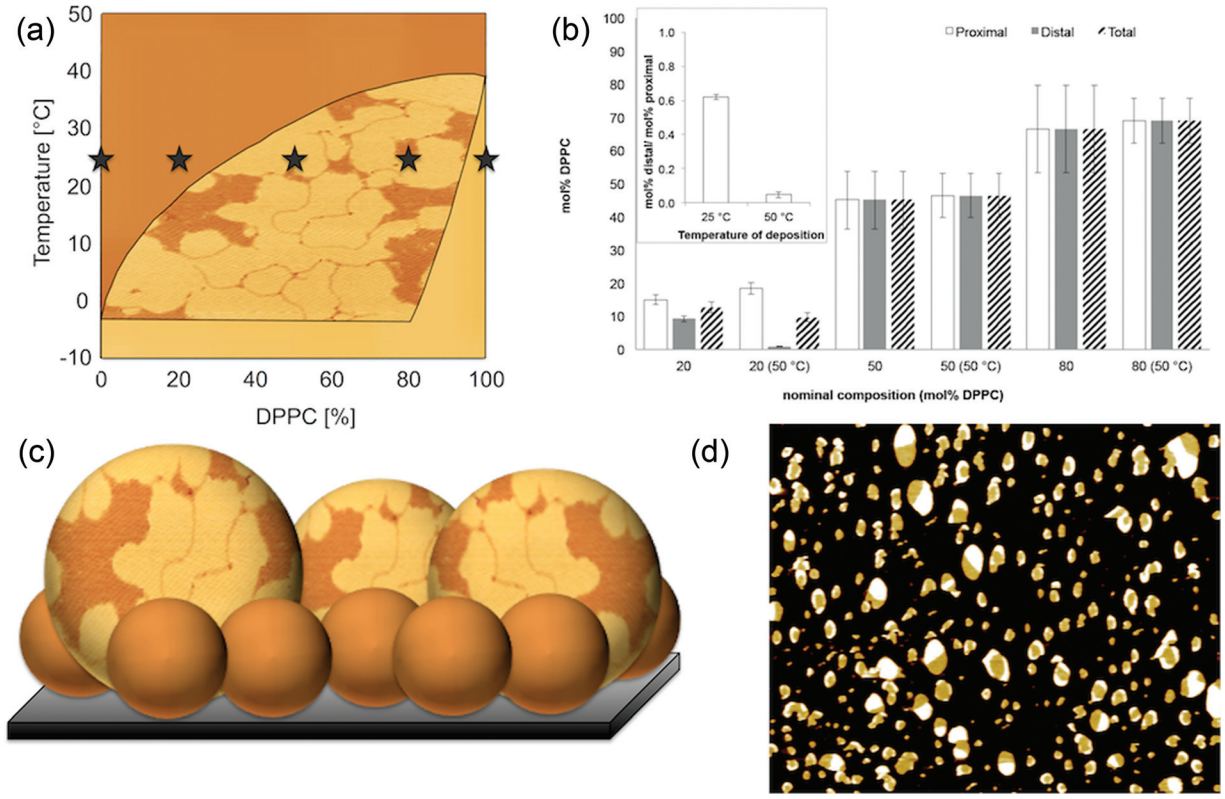

FIG. 6. (a) Phase diagram for aqueous solutions of POPC and DPPC, redrawn from Shoemaker *et al*. (Ref. 60) The black stars denote the lipid ratios of POPC and DPPC at 25 °C that were studied by Åkesson *et al*. (Ref. 11) The dark brown color marks the single-phased fluid region of the phase diagram whereas the lighter color marks the gel-like single-phased region. Fluid domains enriched in POPC coexist with gel-like domains enriched in DPPC in the phase-separated region in the middle. The background of the coexistence region is an AFM image of an 80 mol. % DPPC membrane. (b) Leaflet composition (mol. % DPPC) as a function of nominal composition (mol. % DPPC). SLBs from POPC and DPPC mixtures show a different composition than the nominal composition of the vesicles. The inset shows the asymmetry as the ratio of distal leaflet mol. % DPPC to proximal leaflet mol. % DPPC as a function of the deposition temperature. (c) Small vesicles were enriched in fluid POPC (dark color), whereas larger vesicles displayed phase separation (light color: DPPC). The small size and high curvature of the fluid vesicles facilitate faster movements and fusion at the surface. (d) AFM image showing that for the 80 mol. % DPPC sample small vesicles were enriched in POPC and larger vesicles were phase-separated. (b) and (d) reproduced with permission from A. Åkesson, T. Lind, N. Ehrlich, D. Stamou, H. Wacklin, and M. Cárdenas, "Composition and structure of mixed phospholipid supported bilayers formed by POPC and DPPC," Soft Matter **8**(20), 5658 (2012).

20 mol. % DPPC sample. Small vesicles in the bulk can display a high degree of inhomogeneity at the single vesicle level within a sample preparation.[63] For vesicles smaller than 25 nm in radius, the compositional differences can reach up to 60%.[63] This vesicle size is within the typical size range of tip-sonicated vesicles.[11] It is thus expected that for the 20 mol. % DPPC sample, a certain population of small vesicles may contain mostly POPC while larger vesicles contain a mixture of both lipids [Fig. 6(c)]. Due to geometrical reasons, fluid POPC lipids should accommodate the larger curvature of smaller vesicles better than the stiffer, cylindrical DPPC molecules. Indeed, AFM imaging of the phase separated 80 mol. % DPPC sample confirmed that bilayer patches corresponding from rupture of the smallest vesicles in the population were in the fluid phase, while patches from larger vesicles showed coexisting phases [Fig. 6(d)]. The overall enrichment of POPC in the SLBs is thus likely to arise from (1) a natural depletion of DPPC in the smallest vesicles and (2) a faster diffusion and a higher propensity of fusion for the small vesicles enriched in POPC than for larger, phase separated vesicles. The degree of POPC enrichment of the phase-separated mixtures depended on the positioning of the nominal composition in the phase diagram [Figs. 6(a) and 6(b)]. The deviation from the nominal composition is therefore proposed to be a result of the compositional and size differences at the single vesicle level. Only the fluid single-phased 20 mol. % DPPC sample showed an asymmetric composition with enrichment of DPPC in the proximal leaflet [Fig. 6(b)]. The reason for asymmetric SLBs is expected to stem from an inherent asymmetry in the bulk vesicles. Due to geometrical reasons it is both entropically and energetically favored for DPPC to preferentially locate in the outer leaflet of the small vesicles, leading to enrichment in the proximal leaflet of the bilayer once fused on the surface. Leaflet asymmetry was also previously observed for other binary mixtures of PC lipids of low and high melting temperature,[55,56] and for binary mixtures of fluid lipids containing charged and noncharged species.[54,58] These results revealed that it cannot be implicitly assumed that vesicle preparations are homogeneous and that SLBs formed by mixed liposomes will display identical composition as in the bulk.

VI. OPTIMIZED EXPERIMENTAL CONDITIONS LEAD TO SUCCESSFUL BILAYER FORMATION OF NATURAL LIPID EXTRACTS

Several protocols for extraction of total and polar lipids from native membranes exist. Moreover, there are commercially available sources for lipid extracts derived from *E. coli*, and they are used regularly in various types of studies.[64–67] Back in 1995 Nollert *et al.* adsorbed vesicles of *E. coli* lipids onto silica, and observed using fluorescence microscopy that the vesicles fused upon addition of divalent cations.[68] However, several recent papers have continued studying the formation of SLBs composed of lipids extracted from bacteria (isolated inner[69] and outer membranes,[70] commercially available polar[71–73] and total lipid extracts[74]) by vesicle fusion. From these publications, it is clear that great discrepancies exist in literature as to whether or not vesicle fusion of such complex mixtures can be completed with success on silica surfaces. This is partly a consequence of the methods used to study SLB formation and the structure of the resulting membrane, as well as to the experimental conditions and the method of preparing the lipid vesicles. Recently, complex mixtures of yeast[75] and *E. coli* extracts[76] were successfully deposited on surfaces via the vesicle fusion method, demonstrating the growing interest in and need for advanced biomimetic model systems. In the case of *E. coli* membranes, Domènech *et al.* showed by AFM imaging that bilayers of the polar lipid extracts could be successfully formed via vesicle fusion on mica.[71,73] Others, including Merz *et al.*,[74] found that it was not possible to form complete membranes on SiO_2, while higher bilayer coverage was found for deposition onto TiO_2. Dodd *et al.*[69] concluded that *E. coli* SLBs could be formed only by mixing of these lipids with significant amounts of POPC (an *E. coli* lipid content of 60% or more led to QCM-D responses that showed no indication of vesicle rupture). However, their AFM images confirmed the presence of SLBs with varying degrees of attached vesicles. They also found that SLB formation was improved by elevating the temperature to 35 °C, but in this study, all depositions were done without a fusion promoter. Unsuccessful SLB formation is typically rationalized by the complexity of the total lipid extract that contains the entire range of bacterial lipids and/or that the resulting bilayers adopt a nonplanar geometry. Recently, the condition of vesicle fusion were optimized to successfully form SLB from various types of extracts from *E. coli* using QCM-D.[76] The optimal conditions were found for a lipid concentration of 100 μg/ml in 10 mM TRIS buffer containing 100 mM NaCl and 2 mM $CaCl_2$ (the latter must be added immediately prior to adsorption to avoid vesicle aggregation in solution). Moreover, the use of small tip sonicated vesicles (110 ± 23 nm in average hydrodynamic diameter) was critical to form a SLB of high coverage on silicon oxide.[76] Another important factor to consider is the presence of continuous flow of the sample to ensure sufficient mass transfer to the surface. For *E. coli* lipid vesicles, a rate of 100 μl/min was used in the QCM-D for approximately 30 min and the deposition temperature was kept at 50 °C to enhance the process of vesicle rupture.[76] From the NR data, it was clear that some vesicle coadsorption could still occur therefore leading to larger signals than expected for complete vesicle fusion in the QCM-D. However SLBs of high quality were obtained as verified by QCM-D, NR and AFM. From the NR data, the SLBs were fitted to a total thickness of 41 ± 2 Å.[76] These structural features are similar to membranes made of DPPC (containing two 16:0 chains) in the fluid phase, for which the acyl and head group region was found previously to be 28 ± 1 and 6.8 ± 1 Å, respectively.[12] The typical chain lengths of *E. coli* lipids are 16:0 and 18:1 but the *E. coli* SLBs were approximately 5 Å thinner than standard POPC (16:0–18:1) SLBs.[11] However, *E. coli* lipids also contain cyclic structures such as cyc17:0, which can alter the packing of the bilayer making it less rigid and thinner.[77]

Lipid bilayers of *E. coli* lipids with a specific asymmetric composition containing the long natural lipopolysaccharide moieties in the outer leaflet can be produced using a deposition method based on the Langmuir–Blodgett and Langmuir–Schaefer techniques.[6,78] The main drawback of this approach, however, is that the biomimetic membranes cannot be produced *in situ* at the liquid–solid interface.

Recent NR studies on complex phospholipid extracts from yeast were performed in the presence and absence of ergosterol (see Fig. 7).[75] The authors successfully formed high quality SLBs from both hydrogenated and deuterated lipid extracts using vesicle fusion (the deposition conditions used were 100 mM NaCl, 20 mM $CaCl_2$, 30 min tip sonication at 65 °C, deposition above 50 °C, lipid concentration unspecified). The lipids in the hydrogenated bilayers comprised a high degree of poly-unsaturations while the deuterated lipid mixtures contained mainly monounsaturated fatty acids.[79] Consistent with this, the hydrogenated bilayers were thinner than both commonly used model 1,2-dioleyl-*sn*-glycero-3-phosphocholine (DOPC 18:1 PC) lipid membranes and the deuterated version of the yeast lipid extract. Indeed, hydrogenated SLBs were 6 Å thinner than the deuterated bilayers. Ergosterol was shown to incorporate in the membranes in a symmetric manner, but the lipid composition and level of acyl chain saturation had an effect on the amount of ergosterol present in the two types of membranes (ergosterol content of 5.5 or 14.5 mol. % in deuterated and hydrogenated samples, respectively) and thus the structure and thickness of these bilayers. The presence of ergosterol caused minimal changes to the deuterated bilayers but increased the thickness of hydrogenated SLBs by 3 ± 2 Å. The difference in bilayer thickness was most likely a consequence of the slightly higher content of ergosterol in the hydrogenated SLBs. The model yeast membranes were used to probe the interaction of Amphotericin B and revealed that the interaction was dependent on the level of lipid poly-unsaturation in the SLBs thus evidencing the need for developing protocols for reconstituting cell membrane mimics on solid supports using complex lipid mixtures extracted from natural sources.

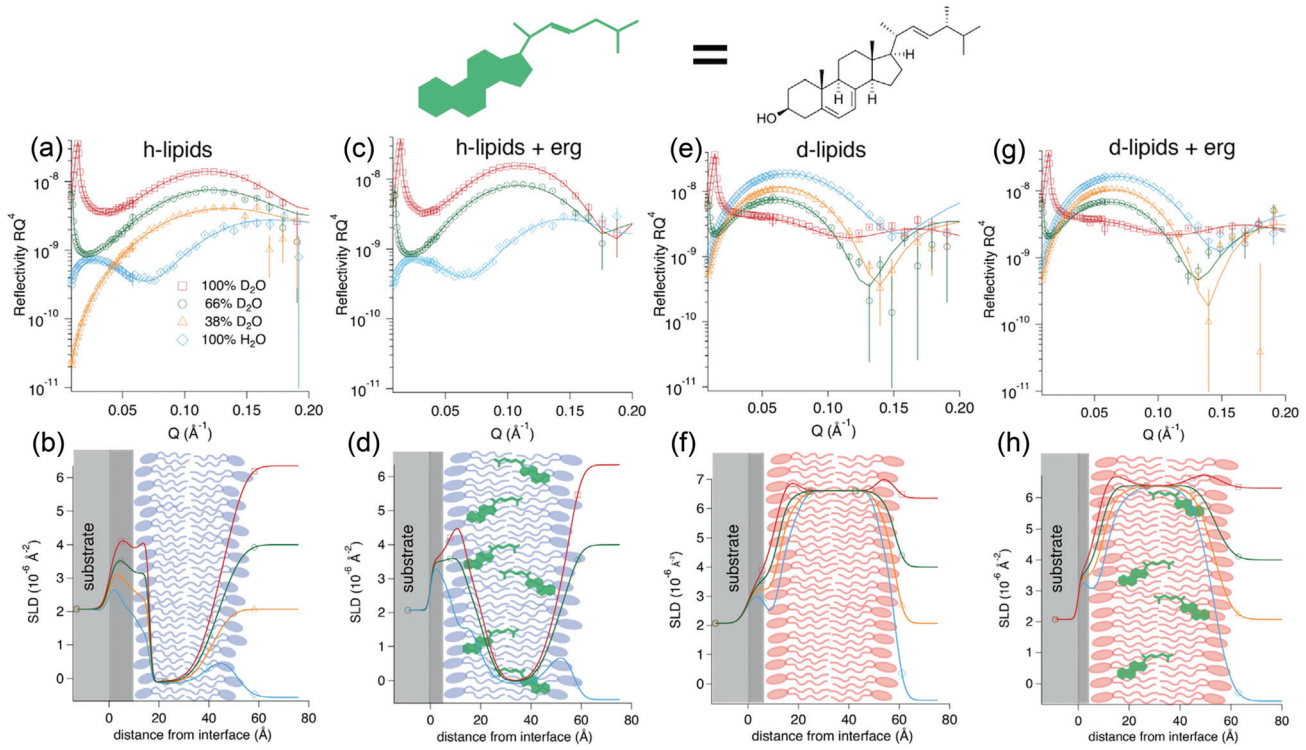

FIG. 7. Neutron reflectivity profiles and corresponding neutron SLD profiles of supported membranes from *Pichia pastoris* lipid extracts using vesicle fusion on silicon substrates in D_2O (red squares), 66% D_2O (green circles), 38% D_2O (orange triangles) and H_2O (blue diamonds): [(a) and (b)] h-lipids [(c) and (d)] h-lipids + ergosterol, [(e) and (f)] d-lipids, and [(g) and (h)] d-lipids + ergosterol. Illustrations of the SLB structures are included in the SLD profiles. Reproduced with permission from A. Ghellinck, G. Fragneto, V. Laux, M. Haertlein, J. Jouhet, M. Sferrazza, and H. Wacklin, "Lipid polyunsaturation determines the extent of membrane structural changes induced by Amphotericin B in Pichia pastoris yeast," Biochim Biophys Acta **1848**(10 Pt A), 2317–2325 (2015).

VII. CONCLUSIONS AND OUTLOOK

The vesicle fusion method, although representing one of the simplest methods for SLB formation, can sometimes be challenging due to the many experimental parameters that influence optimal vesicle rupture and bilayer formation. One major concern is the presence of cobound vesicles. Ideally, for SLBs to be used as biomimetic membrane models in the investigation of molecular interactions, they should be free of attached vesicles. However, depending on the techniques used for studying the interactions, the presence of a small amount of vesicles bound to the SLB does not necessarily affect the experimental design as long as scientists are aware of their presence upon data interpretation. QCM-D, a very sensitive technique to soft layers, might be slightly misleading in this case. A plausible scenario upon interaction with surface active molecules is the stiffening of vesicles, their collapse and the formation of multilayer stacks.[80] Since QCM-D is today considered a method of excellence to optimize the formation of SLBs via vesicle fusion, we would like to bring forward a few factors to consider when interpreting and developing new protocols. We focus on a few key parameters needed to promote vesicle fusion on silica or mica surfaces. Besides the lipid concentration and the presence of flow,[30] the size distribution of the vesicle preparation is critical.[47] It has been shown that successful vesicle fusion of PC vesicles can only be obtained for vesicles with average hydrodynamic diameters of $\leq$90 nm as evaluated by QCM-D.[47,76] For PC binary mixtures we have shown that fusion occurred for vesicles with a diameter of $\leq$50 nm as evaluated by QCM-D, NR and AFM.[11] Vesicles from *E. coli* total lipid extracts successfully formed SLBs for vesicles with an average hydrodynamic diameter of $\leq$110 nm. This smaller size distribution is sometimes easier to achieve in pure water rather than salt or buffer-containing solutions both for tip sonication and extrusion. Furthermore, increasing the deposition temperature can facilitate vesicle fusion. However, for lipids of high T_m, lipid deposition above the melting temperature can also affect the bilayer quality in terms of lowering of the SLB coverage, due to shrinking of the bilayer upon undergoing a transition back to the fluid phase.[12] An alternative is to form the SLB below the T_m and then expose the membrane to a careful rinse with hot water or buffer. In such cases, individual optimizations of the solution conditions and rinsing steps are needed in order to promote the removal of attached vesicles, e.g., by subjecting them to osmotic shock.[34,54] QCM-D studies indicate that it is rarely possible to form SLBs on substrates such as gold;[31,50] however, neutron reflection has demonstrated that high quality SLBs can be formed on gold via the vesicle fusion method.[45] Finally, for vesicle preparations containing more than one lipid species, the resulting SLBs might not have the same composition and structure as the vesicles they were made from.[13,55–58] Thus, QCM-D studies must be complemented

with a secondary surface sensitive technique that either probes the optical properties of the interface (ellipsometry/surface plasmon resonance/reflectometry) or the morphology of the interface (AFM). For detailed compositional analysis, NR and spectrosocopic based techniques are the methods of choice.

ACKNOWLEDGMENTS

The authors gratefully acknowledge financial support from the Center for Synthetic Biology "bioSYNergy" supported by the UCPH Excellence Program for Interdisciplinary Research and the Swedish Research Council. Thanks to funding from Plant Power: Light driven synthesis of complex terpenoids using cytochrome P450s funded by the Innovation Fund Denmark.

[1]M. Eeman and M. Deleu, Biotechnol. Agron. Soc. **14**, 719 (2010), available at http://popups.ulg.ac.be/1780-4507/index.php?id=6568.
[2]Y. H. Chan and S. G. Boxer, Curr. Opin. Chem. Biol. **11**, 581 (2007).
[3]T. G. Pomorski, T. Nylander, and M. Cardenas, Adv. Colloid Interface Sci. **205**, 207 (2014).
[4]K. B. Blodgett, J. Am. Chem. Soc. **57**, 1007 (1935).
[5]A. V. Hughes, S. J. Roser, M. Gerstenberg, A. Goldar, B. Stidder, R. Feidenhans'l, and J. Bradshaw, Langmuir **18**, 8161 (2002).
[6]L. A. Clifton, M. W. Skoda, E. L. Daulton, A. V. Hughes, A. P. Le Brun, J. H. Lakey, and S. A. Holt, J. R. Soc. Interface **10**, 2013081 (2013).
[7]H. P. Vacklin, F. Tiberg, and R. K. Thomas, Biochim. Biophys. Acta **1668**, 17 (2005).
[8]M. Ollivon, S. Lesieur, C. Grabielle-Madelmont, and M. Paternostre, Biochim. Biophys. Acta **1508**, 34 (2000).
[9]R. P. Richter and A. R. Brisson, Biophys. J. **88**, 3422 (2005).
[10]R. Richter, A. Mukhopadhyay, and A. Brisson, Biophys. J. **85**, 3035 (2003).
[11]A. Åkesson, T. Lind, N. Ehrlich, D. Stamou, H. Wacklin, and M. Cárdenas, Soft Matter **8**, 5658 (2012).
[12]T. K. Lind, M. Cardenas, and H. P. Wacklin, Langmuir **30**, 7259 (2014).
[13]V. Rondelli, G. Fragneto, S. Motta, E. D. Favero, and L. Cantù, J. Phys.: Condens. Ser. **340**, 012083 (2012), available at http://stacks.iop.org/1742-6596/340/i=1/a=012083.
[14]K. Funakoshi, H. Suzuki, and S. Takeuchi, Anal. Chem. **78**, 8169 (2006).
[15]G. J. Taylor and S. A. Sarles, Langmuir **31**, 325 (2015).
[16]W. L. Hwang, M. Chen, B. D. Cronin, M. A. Holden, and H. Bayley, J. Am. Chem. Soc. **130**, 5878 (2008).
[17]A. Fischer, M. A. Holden, B. L. Pentelute, and R. J. Collier, Proc. Natl. Acad. Sci. U.S.A. **108**, 16577 (2011).
[18]L. Bradshaw, RF Time Freq. **8**, 50 (2008).
[19]Biolin Scientific, Q-Sense Sensors.
[20]K. K. Kanazawa and J. G. Gordon, Anal. Chim. Acta **175**, 99 (1985).
[21]G. Sauerbrey, Z. Phys. **155**, 206 (1959).
[22]M. Rodahl, F. Hoüoük, A. Krozer, P. Brzezinski, and B. Kasemo, Rev. Sci. Instrum. **66**, 3924 (1995).
[23]A. Mechler, S. Praporski, K. Atmuri, M. Boland, F. Separovic, and L. L. Martin, Biophys. J. **93**, 3907 (2007).
[24]M. V. Voinova, M. Rodahl, M. Jonson, and B. Kasemo, Phys. Scr. **59**, 391 (1999).
[25]D. D. Joseph, *Fluid Dynamics of Viscoelastic Liquids* (Springer, New York, 1990).
[26]E. Tellechea, D. Johannsmann, N. F. Steinmetz, R. P. Richter, and I. Reviakine, Langmuir **25**, 5177 (2009).
[27]Q-Sense, "Quartz crystal microbalance with dissipation monitoring (QCM-D)," Q-sense Technology Note: QS 407-01-2 (2014).
[28]C. Striebel, A. Brecht, and G. Gauglitz, Biosens. Bioelectron. **9**, 139 (1994).
[29]F. Höök, B. Kasemo, T. Nylander, C. Fant, K. Sott, and H. Elwing, Anal. Chem. **73**, 5796 (2001).
[30]N. J. Cho, C. W. Frank, B. Kasemo, and F. Hook, Nat. Protoc. **5**, 1096 (2010).
[31]K. F. Wang, R. Nagarajan, and T. A. Camesano, Biophys. Chem. **196**, 53 (2015).
[32]N. Y. Lu, K. Yang, J. L. Li, B. Yuan, and Y. Q. Ma, Biochim. Biophys. Acta **1828**, 1918 (2013).
[33]N. Lu, K. Yang, B. Yuan, and Y. Ma, J. Phys. Chem. B **116**, 9432 (2012).
[34]E. Reimhult, F. Höök, and B. Kasemo, Langmuir **19**, 1681 (2003).
[35]J. A. Zasadzinski, C. A. Helm, M. L. Longo, A. L. Weisenhorn, S. A. Gould, and P. K. Hansma, Biophys. J. **59**, 755 (1991).
[36]Q. Zhong, D. Inniss, K. Kjoller, and V. B. Elings, Surf. Sci. **290**, L688 (1993).
[37]Bruker Nano Surfaces Divison, "Quantitative mechanical property mapping at the nanoscale with PeakForce QNM," Application Note No. 128 (2012).
[38]M. P. Mingeot-Leclercq, M. Deleu, R. Brasseur, and Y. F. Dufrene, Nat. Protoc. **3**, 1654 (2008).
[39]T. K. Lind, P. Zielinska, H. P. Wacklin, Z. Urbanczyk-Lipkowska, and M. Cardenas, ACS Nano **8**, 396 (2014).
[40]G. Fragneto, Eur. Phys. J.: Spec. Top. **213**, 327 (2012).
[41]G. Fragneto-Cusani, J. Phys.-Condens. Matter **13**, 4973 (2001).
[42]S. Maric *et al.*, Appl. Microbiol. Biotechnol. **99**, 241 (2015).
[43]T. Salditt, Curr. Opin. Struct. Biol. **13**, 467 (2003).
[44]I. Burgess, M. Li, S. L. Horswell, G. Szymanski, J. Lipkowski, J. Majewski, and S. Satija, Biophys. J. **86**, 1763 (2004).
[45]R. P. Richter, R. Berat, and A. R. Brisson, Langmuir **22**, 3497 (2006).
[46]B. Seantier, C. Breffa, O. Felix, and G. Decher, J. Phys. Chem. B. **109**, 21755 (2005).
[47]Y. Jing, H. Trefna, M. Persson, B. Kasemo, and S. Svedhem, Soft Matter **10**, 187 (2014).
[48]T. K. Lind, "Understanding peptide dendrimer interactions with model cell membrane mimics," Ph.D. thesis (Copenhagen University, 2014).
[49]C. A. Keller and B. Kasemo, Biophys. J. **75**, 1397 (1998).
[50]B. Seantier, C. Breffa, O. Félix, and G. Decher, Nano Lett. **4**, 5 (2004).
[51]M. Beckmann, P. Nollert, and H. A. Kolb, J. Membr. Biol. **161**, 227 (1998).
[52]E. Reimhult, F. Hook, and B. Kasemo, J. Chem. Phys. **117**, 7401 (2002).
[53]C. A. Keller, K. Glasmastar, V. P. Zhdanov, and B. Kasemo, Phys. Rev. Lett. **84**, 5443 (2000).
[54]S. Stanglmaier, S. Hertrich, K. Fritz, J. F. Moulin, M. Haese-Seiller, J. O. Rädler, and B. Nickel, Langmuir **28**, 10818 (2012).
[55]H. P. Wacklin, Langmuir **27**, 7698 (2011).
[56]H. P. Wacklin and R. K. Thomas, Langmuir **23**, 7644 (2007).
[57]W. C. Lin, C. D. Blanchette, T. V. Ratto, and M. L. Longo, Biophys. J. **90**, 228 (2006).
[58]F. F. Rossetti, M. Textor, and I. Reviakine, Langmuir **22**, 3467 (2006).
[59]R. P. Richter, N. Maury, and A. R. Brisson, Langmuir **21**, 299 (2005).
[60]S. D. Shoemaker and T. K. Vanderlick, Biophys. J. **84**, 998 (2003).
[61]W. Curatolo, B. Sears, and L. J. Neuringer, Biochim. Biophys. Acta **817**, 261 (1985).
[62]H. A. Rinia and B. de Kruijff, FEBS Lett. **504**, 194 (2001).
[63]J. Larsen, N. S. Hatzakis, and D. Stamou, J. Am. Chem. Soc. **133**, 10685 (2011).
[64]G. F. White, K. I. Racher, A. Lipski, F. R. Hallett, and J. M. Wood, Biochim. Biophys. Acta. **1468**, 175 (2000).
[65]I. Lopez-Montero, L. R. Arriaga, G. Rivas, M. Velez, and F. Monroy, Chem. Phys. Lipids. **163**, 56 (2010).
[66]E. J. Prenner, R. N. Lewis, K. C. Neuman, S. M. Gruner, L. H. Kondejewski, R. S. Hodges, and R. N. McElhaney, Biochemistry **36**, 7906 (1997).
[67]C. Roos *et al.*, Biochim. Biophys. Acta **1818**, 3098 (2012).
[68]P. Nollert, H. Kiefer, and F. Jahnig, Biophys. J. **69**, 1447 (1995).
[69]C. E. Dodd, B. R. Johnson, L. J. Jeuken, T. D. Bugg, R. J. Bushby, and S. D. Evans, Biointerphases **3**, FA59 (2008).
[70]N. Ruiz, S. Merino, M. Vinas, O. Domenech, M. T. Montero, and J. Hernandez-Borrell, Biophys. Chem. **111**, 1 (2004).
[71]S. Merino, Ò. Domènech, I. Díez, F. Sanz, M. Viñas, M. T. Montero, and J. Hernández-Borrell, Langmuir **19**, 6922 (2003).
[72]S. Garcia-Manyes, G. Oncins, and F. Sanz, Biophys. J. **89**, 1812 (2005).
[73]Ò. Domènech, S. Merino-Montero, M. T. Montero, and J. Hernandez-Borrell, Colloids Surf., B **47**, 102 (2006).
[74]C. Merz, W. Knoll, M. Textor, and E. Reimhult, Biointerphases **3**, FA41 (2008).
[75]A. de Ghellinck, G. Fragneto, V. Laux, M. Haertlein, J. Jouhet, M. Sferrazza, and H. Wacklin, Biochim. Biophys. Acta **1848**, 2317 (2015).

[76]T. K. Lind, H. Wacklin, J. Schiller, M. Moulin, M. Haertlein, T. G. Pomorski, and M. Cardenas, PLoS One **10**, e0144671 (2015).
[77]K. R. Pandit and J. B. Klauda, Biochim. Biophys. Acta **1818**, 1205 (2012).
[78]L. A. Clifton *et al*., Angew. Chem. Int. Ed. Engl. **54**, 11952 (2015).
[79]A. de Ghellinck, H. Schaller, V. Laux, M. Haertlein, M. Sferrazza, E. Maréchal, H. Wacklin, J. Jouhet, and G. Fragneto, PLoS One **9**, e92999 (2014).
[80]A. Åkesson, C. V. Lundgaard, N. Ehrlich, T. G. Pomorski, D. Stamou, and M. Cárdenas, Soft Matter **8**, 8972 (2012).